Slumped Glass Optics for X-ray telescopes: advances in the hot slumping assisted by pressure

B. Salmaso[*a,b], C. Brizzolari[a,c], S. Basso[a], M. Civitani[a], M. Ghigo[a], G. Pareschi[a], D. Spiga[a], G. Tagliaferri[a], G.Vecchi[a]

[a]INAF/Brera Astronomical Observatory, Via E. Bianchi 46, 23807 Merate, Italy
[b]Università degli Studi dell'Insubria, Via Valleggio 11, 22100 Como, Italy
[c]Università di Milano-Bicocca, piazza della Scienza 3, 20126 Milano, Italy

ABSTRACT

Slumped Glass Optics is a viable solution to build future X-ray telescopes. In our laboratories we use a direct hot slumping approach assisted by pressure, in which the glass optical surface is in contact with the mould, and a pressure is applied to enforce the replication of the mould shape on the glass optical surface. Several prototypes have been already produced and tested in X-rays, showing a continuous improvement in our technology. In this paper, we present the advances in our technology, in terms of slumped glass foils quality and expected performances upon an ideal integration. By using Eagle XG glass foils and Zerodur K20 for the slumping mould, we have fine tuned several process parameters: we present a critical analysis correlating the changes in the process to the improvements in different spatial frequency ranges encompassing the profile and roughness measurements. The use of a re-polished K20 mould, together with the optimized process parameters, lead to the latest result of glass foils with expected performance of less than 3 arcsec in single reflection at 1 keV X-ray energy. This work presents all the relevant steps forward in the hot slumping technology assisted by pressure, aimed at reaching angular resolutions of 5 arcsec for the whole mirror assembly.

Keywords: hot slumping, thin glass mirrors, Zerodur K20, Eagle XG, X-ray segmented optics, astronomical telescopes, Slumped Glass Optics

1. INTRODUCTION

To significantly improve the performances of the current X-ray observatories, the next generation of X-ray telescopes has to be characterized by a large effective area and very small angular resolution. The optics of the ATHENA mission, approved for the L2 slot in the ESA Cosmic Vision program, will have effective area of 2 m^2 at 1 keV and angular resolution better than 5 arcsec [1]. The large dimension implied by these requirements forces the use of a modular approach, splitting the optics into segments. Moreover, lightweight materials have to be selected for the segmented optics in order to maintain a manageable weight for the optics. By now, Silicon Pore Optics (SPO) is considered the baseline technology for this mission. Beside that, the Slumped Glass Optics (SGO) technology is studied both as alternative / hybrid solution for the ATHENA optics and for high precision optics like the SMART-X, which would utilize adjustable optics to achieve Chandra like resolution with 30 times its collecting area [2] and the AXYOM project, which is introducing the coupling of the piezoelectric elements with the reinforcing ribs already used in our integration scheme [3].

The Brera Astronomical Observatory (INAF-OAB) is developing the SGO technology to manufacture the modular elements required for these optics. We are working on the SGO technology since 2009. The research was supported until June 2013 by the European Space Agency (ESA) and proceeded with the collaboration of several institutes and Italian companies: Max Planck Institut für Extraterrestrische Physik (MPE, Garching, Germany), BCV-Progetti (Milano, Italy), ADS-International (Lecco, Italy), and Media Lario Technologies (Bosisio Parini, Italy). The study is still pursued to optimize the SGO technology. In our laboratories we form thin glass foils (0.4 mm thin) by direct hot slumping, assisted by pressure, replicating the shape of a cylindrical mould. The formed foils are then stacked into Wolter-I configuration via a dedicated Integration Machine (IMA), to form the X-ray Optical Unit (XOU), the basic element of the telescope.

[*] bianca.salmaso@brera.inaf.it; phone +39-039-5971028; fax +39-039-5971001; www.brera.inaf.it

Optics for EUV, X-Ray, and Gamma-Ray Astronomy VII, edited by Stephen L. O'Dell, Giovanni Pareschi,
Proc. of SPIE Vol. 9603, 96030O · © 2015 SPIE · CCC code: 0277-786X/15/$18 · doi: 10.1117/12.2187539

Several prototypes, fully produced in our laboratories, have been tested in X-rays at PANTER/MPE, showing a continuous improvement in performances, obtained by optimizing the process at various levels [4]. Moreover, new collaborations, with other groups producing glass foils, were set in order to jointly optimize the SGO. A new prototype, with glass foils produced at MPE with the indirect method, was integrated in our laboratories [5].
In this paper, we present the advances in our technology, in terms of slumped glass foils quality and expected performances upon an ideal integration, first giving an overview of the quality improvements during our research activity, then focusing on the results recently obtained on a newly procured K20 mould.
In section 2, we briefly review the experimental setup and materials used for our hot slumping process, and we give an overview on the development of our technology. In section 3, we describe the metrology used for the characterization in shape and roughness. In section 4, we present the key parameters adopted to optimize the optical quality of the slumped glass foils, by correlating the changes in the process to the improvements in different spatial frequency ranges. A further improvement was obtained with the use of a re-polished K20 mould: in section 5, we present the characterization of this mould, giving special attention to the developed protocols for the annealing and cleaning of this material. In section 6, the quality of the glass foils, slumped on this new K20, is compared to the quality of the glass foils integrated into our most recent prototypes, showing the improvement both in terms of reduced sag error and mid frequency errors: for these new slumped glass foils, the expected performances were proven to be less then 3 arcsec in single reflection at 1 keV X-ray energy. Finally in section 7, we summarize all the results, and we present the conclusions and the outlooks of this research activity.

2. THE DIRECT HOT SLUMPING ASSISTED BY PRESSURE

2.1 The technology

In the hot slumping, the shape of a thin glass foil is modified with a proper thermal cycle in order to replicate the surface of a slumping mould. We use a direct approach, which means that the optical surface of the glass foil is in contact with the mould. In our approach the contact is forced by the application of pressure: the glass foil, slumped with a size larger than the final one, is positioned over the mould inside a stainless still muffle and it divides the muffle chamber in two parts, the lower one being kept at lower pressure, to force the glass foil towards the mould.

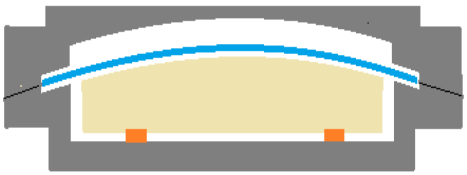

Fig. 1. A flat glass foil is positioned over a cylindrical mould, inside a stainless steel muffle. With this setup, the glass itself can act as a membrane that allows the pressure application.

The materials for both the slumping mould and the glass foil have to be chosen accurately. During our research, we have started by using D263 glass foils combined with Fused Silica for the slumping mould: a detaching layer of Cr+Pt was used on the Fused Silica, but this layer was shown to degrade after several slumping cycle [6]. Therefore the Zerodur K20 was chosen for the slumping mould, being a material that does not need a detaching layer. The glass foil material was then changed from D263 to AF32, both produced by Schott, for the better quality obtained in the slumped glass foils, owing the better coupling of Coefficient of Thermal Expansion (CTE_{K20} = 2.0 10^{-6}/ºK, CTE_{D263} = 7.2 10^{-6}/ºK, CTE_{AF32} = 3.2 10^{-6}/ºK). The good coupling of the CTE of the glass and the mould is, in fact, a key factor for the optical quality of the slumped glass foils, as it avoids the shear of the optical surface on the mould when the temperature is decreased, thereby reducing errors in the centimeter spatial wavelengths. These types of errors are expected to be present on the glass surface, when the glass is in contact with the mould [7], and they have to be minimized as, unlike low frequency errors, they are not corrected by our integration procedure [8] (see sect. 4.1). Finally the Eagle XG, produced by Corning, was adopted for three major reasons:

1) Schott stopped the production of the AF32 in the size required by our setup: in fact the glass foil is slumped with a larger dimension than the final one, to act as a membrane that allows the pressure application (Fig. 1)
2) Eagle XG has a better quality surface in terms of waviness and thickness uniformity [9] which is important when considering the indirect approach [10]

3) Eagle XG is compatible with the technology developed for the SMART-X project: in fact the adopted piezoelectric film (PZT), applied after the slumping process, requires a thermal cycle that reaches T = 550 °C. Early works at SAO – Massachussets, showed that the D263 glass was deforming during the PZT thermal cycle, being the annealing temperature of the glass, T_{D263} = 557 °C, too close to the crystallization temperature of the PZT. For this reason the Eagle XG was chosen, having a higher annealing temperature, T_{Eagle} = 722 °C [11].

In our setup, the glass foil and the mould are positioned in the muffle inside a furnace. For several years, we have adopted a muffle with a light open cover (Fig. 2 – left) to have access to the precious information of the change in the interference fringes between the glass foil and the mould surface during the slumping. Ad hoc windows in the furnace (Fig 2 – center) enable the movie recording (Fig 2 – right).

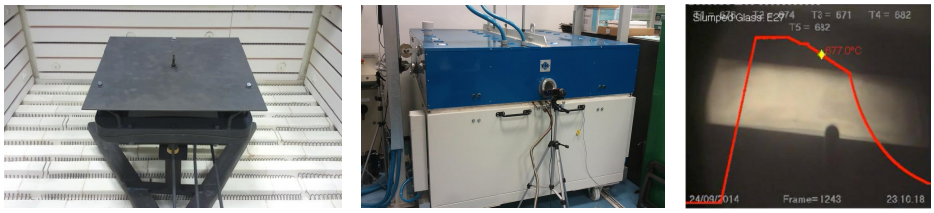

Fig. 2. Left: The muffle with the light open cover. Center: the furnace with the windows for the camera. Right: one shot of the movie of the change in the interference fringes, recorded during the slumping cycle.

The thermal cycle (red line in Fig. 2 – right) foresees a ramp-up from room temperature to T_{max} = 750 °C, a soaking time of 4 h at T_{max} and a cooling cycle sufficiently slow to let the glass foil the time to relax in order to minimize the mid frequency errors. The use of the pressure was proven to be a key parameter to reduce the mid frequency errors in the slumped glass foils [12]. The 50 g/cm^2 value was determined by a trade off between the minimization of the mould roughness replication into the glass foil and the minimization of the amplitude of the shape errors in the cm frequency range.

2.2 The development of our technology: trend in the prototypes performances

The first prototype of SGO, the Proof of Concept #1 (PoC#1), was produced using 0.4 mm thick Schott D263 glass foils, slumped on a Pt-coated Fused Silica cylindrical mould [6]. The resulting Half Energy Width (HEW) was 80 arcsec, affected by a high surface roughness, because of the utilization of a metal membrane for pressure application and poorly shaped integration moulds in Metapore, a material difficult to precisely figure.
The subsequent prototype, XOU-BB (X-Ray Optical Unit Bread Board) was then realized with D263 glass foils slumped on moulds of different materials and using different settings for the application of pressure [13]. Its main goal was to manufacture a complete optical unit model of the IXO optical system, demonstrating in particular the capability of stacking of plate pairs with the IMA.
A later prototype (PoC#2) was produced with Schott AF32 glasses slumped on a Zerodur K20 mould. A better matching of the Coefficient of Thermal Expansion (CTE) of the two materials has produced better results in the slumped glass foils. Moreover newly procured BK7 integration moulds, with much more accurate Wolter-I profiles with respect to the previous Metapore moulds, were used for the integration of these glass foils. These modifications have allowed the complete module to reach a HEW of ~ 22 arcsec and the better plate pair a HEW of ~ 20 arcsec, directly measured in-focus at 0.27 keV at the PANTER facility [4].
The next prototype (PoC#3) was realized with Corning Eagle glass foils, slumped on a newly procured K20 mould, with homogeneous highly reflective surface in order to reduce the errors in the cm/mm range. Actually, since the beginning of 2014, we have used two different slumping moulds in Zerodur K20. The first one, hereafter called MK20-10, was used for the production of the PoC#2 glass foils. A thorough slumping process optimization was carried out on the MK20-10 mould. The glass material was changed to Corning Eagle XG, the soaking time was increased and the mould height was changed to start with glass-to-mould contact at room temperature. These conditions were in fact defined as effective to reduce the sag error and the profile variability from glass to glass. While optimizing the process, a second mould, MK20-20, was produced. Fig. 3 shows the poor reflectivity of the MK20-10 with respect to the MK20-20: a pattern in the change of reflectivity is seen for the MK20-10, affecting the slumped glass foils in the spatial frequencies range of the

cm/mm. It is therefore clear that the reduction of these errors in the slumped glass foils could be reached only on the MK20-20.

Fig. 3. Visual comparison of the surface roughness of the MK20-10 and MK20-20 (size 250 mm x 250 mm). Left) the MK20-10 shows the optical part (200mm x 200mm) with lower reflectivity due to a damaged surface. Patterns are also visible on the surface. Right) the MK20-20 with the homogeneous highly reflective surface.

It was found that the process could not be transferred directly from MK20-10 to MK20-20, as the different shearing of the glass foil on the rough or smooth surface was producing different technical issues to be solved. In particular, the starting with glass-to-mould contact at room temperature, optimal with a rough mould surface, was found to lead to air bubble entrapping with a smooth mould surface, the higher glass-to-mould contact giving less space for the air to flow out of the contact area during the slumping cycle. To avoid air bubbles, the pressure was applied at room temperature rather than after the reaching of the slumping temperature: while effective in avoiding air bubbles, this lead to an increase in sag error with respect to the improved results already obtained on MK20-10 after the POC#2, the sag error of the slumped glass foils integrated into the PoC#3 being approximately the same as the one of the POC#2 glass foils [4]. The overall HEW of the PoC#3 was found to be higher with respect to the PoC#2 ($HEW_{POC\#3}$ = 30 arcsec, $HEW_{POC\#2}$ = 22 arcsec) was most likely due to asymmetric deformations of the K20 due to preliminary slumping cycles that suffered from air entrapping in the central region [12] and from some deformations in the slumped glass foils due to entrapped dust during the slumping. Nevertheless the best HEW value, in a portion of the module, was 5.5 arcsec at 0.27 keV [4], thank to the use of the new K20. Moreover, the impact of the roughness in the 0.27-1.49 keV range was considerably reduced with respect to the previous prototypes, thanks to the better surface roughness of the MK20-20.
The lesson learnt from the PoC#3 was that a further work was necessary to reduce the sag error of the slumped glass foils. The soaking time was therefore increased over the 4h, used for the PoC#3 glass foils production. Before reaching the necessary decrease in sag, we had a glass foil sticking onto the K20 surface.
A rework of the MK20-20 mould was therefore necessary. The re-polished mould was named MK20-20B. While the MK20-20 was re-worked, an accurate analysis of various parameters was done on the MK20-10 mould, with the aim to reducing the sag error, the mid frequencies and the roughness (sect. 4-5). The mould height was optimized with Finite Element Analysis and experiments; the muffle was closed to reduce the thermal gradients; the cooling rate were decreased; a new protocol for cleaning the mould surface before slumping was introduced, in order to avoid repetitive spots at subsequent slumping cycles.
The best glass foils produced on the MK20-10 during this research activity, were integrated into the prototype PoC#4. Despite we expected an HEW of about 15 arcsec from metrological data, the result in X-ray was much higher [14]. Since we believe that this is most probably due to an integration error, the prototype will be disassembled an re-integrated into a PoC#5, together with the best glass foils slumped on the re-polished MK20-20B, showing the best quality obtained so far (sect. 6).

3. THE METROLOGY

3.1 The roughness metrology

The surface roughness of the slumped glass foils is routinely characterized, in our laboratories, with the WYKO Phase Shift Interferometer and the Atomic Force Microscope (AFM). With these instruments we can measure the surface roughness in a large range of spatial frequencies, going from 5.2 mm (the scan length of the WYKO interferometer with the 2.5X objective) down to 0.05 μm with the AFM at scan length 10 μm. In Fig.4 we show the roughness of one glass foil slumped on the new MK20-20B: the partial replication of the mould roughness guarantees a contribution from roughness to the final HEW of less then 1 arcsec at 1 keV.

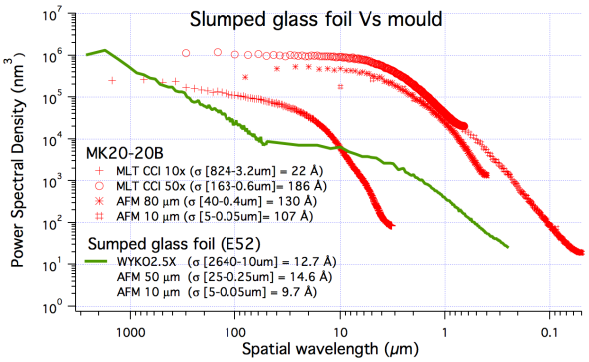

Fig. 4. PSD from roughness data obtained for the MK20-20B slumping mould (red line) and one Eagle glass foil slumped on it (green line, glass code E52).

3.2 The shape metrology

The shape of the glass foils and moulds are routinely characterized in our laboratories with the Long Trace Profilometer for 1-D profiles and with the Characterization Universal Profilometer (CUP) for 2-D maps [15]. These instruments give a substantial difference on the mid frequency contribution, especially at the azimuthal coordinates more distant from the centre, both for the glass foils and the moulds, where the LTP returns expected HEW values much lower than the CUP: on MK20-20B, at a position 80 mm off the centre, the expected HEW computed from longitudinal profiles after the subtraction of 8th order polynomials are $HEW_{CUP} \sim 8$ arcsec and $HEW_{LTP} \sim 1$ arcsec. To discriminate the result, a third instrument was used: the ZYGO interferometer available at our laboratories was used with a flat null lens of 100 mm diameter, therefore returning only mono-dimensional profiles of 100 mm maximum length of the cylindrical surfaces of slumping moulds and glass foils. Since the measurements on glass foils are more difficult because the samples are sensitive to vibrations, we have scanned the MK20-20B slumping mould on three positions to compare them with the LTP data: the center, 80 mm right from center, 80 mm left from center. Fig. 5 shows one of the three profiles obtained after the subtraction of the best fit 8th order polynomial: the LTP and ZYGO measurements are in very good agreement, the small differences of about 10 nm being due to:

- alignment errors: small deviation from the azimuthal coordinate would result in a comparison of slightly different profiles with differences in mid frequency height contribution
- lower accuracy and repeatability of the LTP with respect to the ZYGO (repeatability over 100 mm at 1 sigma: rms-LTP = 5 nm, rms-ZYGO=1nm).

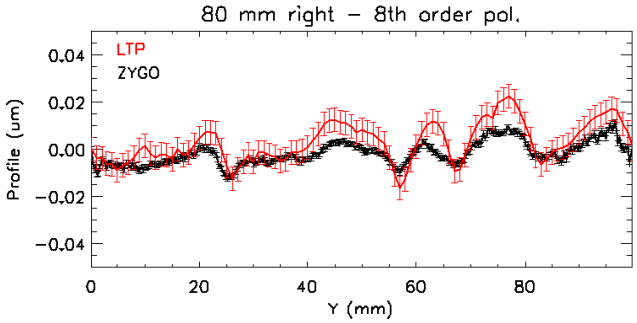

Fig. 5. Comparison between the LTP (red curve) and ZYGO (black curve) scans of the MK20-20B after annealing: the profile shown was taken at 80 mm right from the center, and it is the residual after the subtraction of the best-fit 8th order polynomial.

In Table 1, the expected HEWs, computed for the three scans, are presented: the results of the LTP and ZYGO data are in substantial agreement with each other and anyway much smaller than what computed with the CUP at position 80 mm off the center (HEW_{CUP} ~ 8 arcsec).

Table 1: HEW computed with physical optics from the LTP and ZYGO scans of the MK20-20B mould after the annealing, after the subtraction of the best fit 8th order polynomial are shown.

	LTP Data - 8th order pol.	ZYGO Data - 8th order pol.
80L	0.13	0.13
C	0.36	0.13
80R	1.4	0.13

Therefore in this paper, all the expected HEWs are presented from data taken with the LTP. The LTP measurements on glass foils are performed routinely on five longitudinal scans [9]: the central scans, two scans 45 mm off the center and two scans 86 mm off the center. A thin layer of First Contact (by Photonic Cleaning) is used to suppress the reflection of the back surface of the glass foil. The deformation of the glass foil due to the gravity and the supporting mounting is removed by Finite Element Analysis (FEA).

4. SLUMPING PROCESS TUNING ON MK20-10

In this paragraph we focus on the metrological results obtained on the slumped glass foils, and the expected HEW in X-rays from simulation. The results obtained after the integration process, with both optical and X-rays characterizations, can be found elsewhere [4,14].

4.1 The importance of the sag error reduction

As already described in section 1, we first produce glass foils with cylindrical shape by hot slumping assisted by pressure and then we impart the correct Wolter-I configuration by forcing the slumped glass foils to replicate the integration moulds, different from the slumping mould, with the use of reinforcing ribs glued to the glass foils [15]. The procedure allows to correct both for the difference from cylinder to Wolter-1 and for residual low frequency errors due to the slumping process, the capability to correct dropping as the errors frequency increases [8]. Finite Element Analysis was carried out in order to compute the correction factors [8] by which we can simulate the integration on the glass foils, assuming perfect integration moulds and no effects due to the glue shrinkage. It was derived that the first harmonic is damped by about 80%; therefore the sag error, despite being efficiently corrected, still needs to be kept at low as possible in order to minimize the final expected HEW.
As already described in section 2.2, the glass foils integrated in the PoC#3 in 2013, the first one realized with Corning Eagle glass foils slumped on a MK20-20, were characterized by a sag error of about 10 μm [4], similar to the one of the glass foils integrated in the PoC#2 in 2012. The research was therefore driven by the need of reducing the sag error of the slumped glass foils. The process changes for this optimization are described in section 4.2. We here want to point out the effect of the sag error reduction into the expected profiles of the integrated glass foils. In Fig. 6 we compare the CUP maps of one glass foil integrated into the PoC#3 (left, central sag error ~ 10 μm) with one glass foil integrated into the PoC#4 and produced with the optimized process (right, central sag error ~ 2 μm). In Fig. 7 we compare the maps of the same glass foils after the simulation of the ideal integration with the use of our damping coefficients. The map of Fig. 7-right clearly shows the benefits of the reduced sag error of this glass foil.

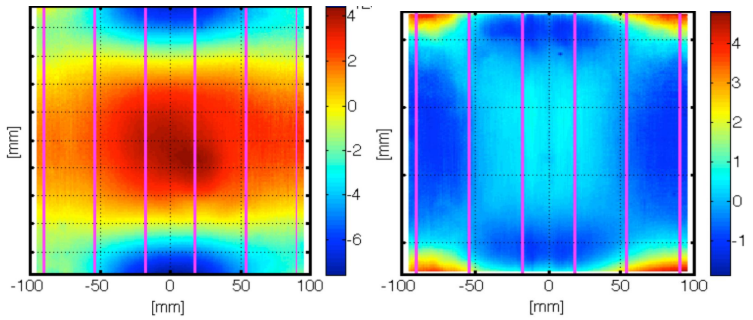

Fig. 6. CUP maps of slumped glass foils: residual with respect of a linear fit along the optical axis (vertical in the figure), at different azimuthal coordinates. The vertical scale is in μm. Left: a glass foil integrated into the PoC#3 (glass code E18, central sag error ~ 10 μm); Right: a glass foil integrated into the PoC#4 (glass code E34, central sag error ~ 2 μm).

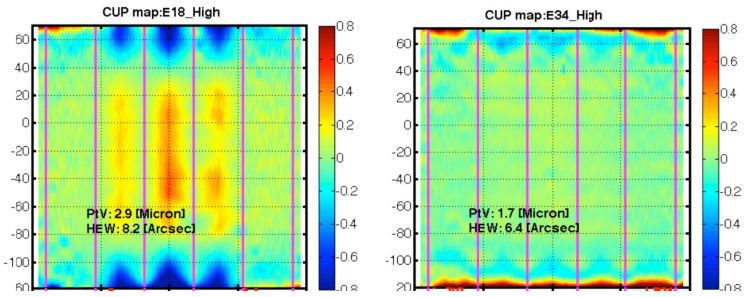

Fig. 7. CUP maps of the same slumped glass foils of Fig. 6, after the simulation of the ideal integration. The vertical scale is in μm. Left: a glass foil integrated into the PoC#3 (glass code E18); Right: a glass foil integrated into the PoC#4 (glass code E34).

As pointed out in section 3.2, we compute the HEWs on five longitudinal LTP scans (green dashed lines of Fig. 8-left) at different distance from the ribs (pink solid lines of Fig. 8-left). The HEWs are computed from physical optics [16] in single reflection from the slumped glass foils data after the simulation of the ideal integration. Fig. 8-right shows the result of this computation for the glass foil E34, integrated into the PoC#4. The HEW values are roughly constant along the five scans, this being an indication of higher frequency errors in the lateral portion of the slumped glass foils. In fact, the closest to the ribs a longitudinal line is, the most efficient the correction during the integration should be, being the elastic shape retrieving of the slumped glass foil to its original shape maximum in between two ribs. We should therefore expect HEW values lower at the lateral scans, while in this case the replication of the surface of the MK20-10, mostly damaged in the lateral portions, is dominating the result. A further reduction of higher frequency errors, in the slumped glass foils, was obtained with the introduction of the re-polished MK20-20B (see section 6).

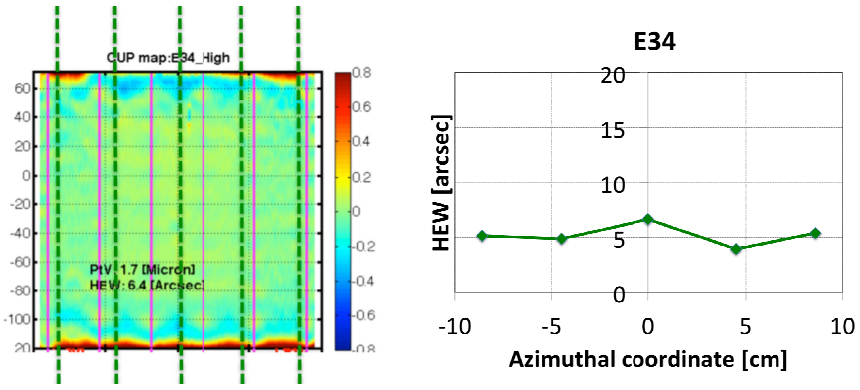

Fig. 8. Left: The green dashed lines show the LTP scan positions over the CUP map of the E34 glass foil, after the simulation of the ideal integration. The pink lines represent the ribs positions. Right: the HEWs computed from the 5 LTP scans, after the simulation of the ideal integration, for the E34 glass foil.

4.2 The optimizes process parameters

While reworking the MK20-20, we have started a campaign to find alternative parameters with respect to the ones adopted for the glass foils integrated into the PoC#3, the goal being to avoid air bubbles entrapping, reduce the sag error and the mid to high frequency errors. The following results were found on the MK20-10 mould:

1) the best height of the mould, with respect to the muffle, was defined by FEA to be an intermediate position between the 0 mm used for the PoC#2 (no glass-to-mould contact at room temperature) and the 2.5 mm used for the PoC#3 (glass-to mould contact already at room temperature) (Fig. 9). The optimal position was defined to be the one where the glass is almost in contact with the mould at the soaking temperature, considering the muffle thermal expansion and the thickness reduction, at high temperature, of the sealing material we use to enable the pressure application (Superwool 607 HT, by Thermal Ceramics).

Fig. 9.: Sketch of the mould and glass foil inside the muffle. The gray spacers represent the sealing material we use to enable the pressure application. From left: the mould is at 0 level with respect to the muffle (PoC#2). The mould is in contact at room temperature with the glass foil (PoC#3). The mould is at an intermediate position defined with FEA (PoC#4)

2) the typical muffle configuration used until the PoC#3 (Fig. 10, left) was enabling us to record the movie of the interference fringes between the glass foil and the mould surface during the slumping. This possibility endowed us with informations about the slumping of the glass foil, like the moment of glass-to-mould contact and the retrieving of the glass rigidity. Nevertheless, in order to further reduce the longitudinal sag error, a muffle cover with cylindrical design at the interior (Fig. 10, right) was then used, which prevented the movie recording, but lead to a reduction in the central longitudinal sag error (Fig. 11, Fig. 12-left).

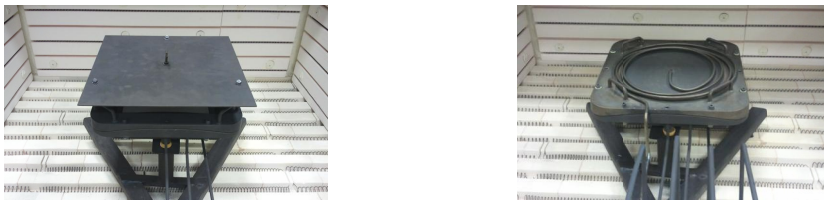

Fig. 10.: Pictures of the muffle inside the oven. Left: the configuration used for all slumped glass foils until the PoC#3 included, enabling the recording of the interference fringes between the glass foil and the mould. Right: the cover with internal cylindrical curvature is used to close the muffle, leading to reduced central sag error (Fig. 11, Fig. 12-left).

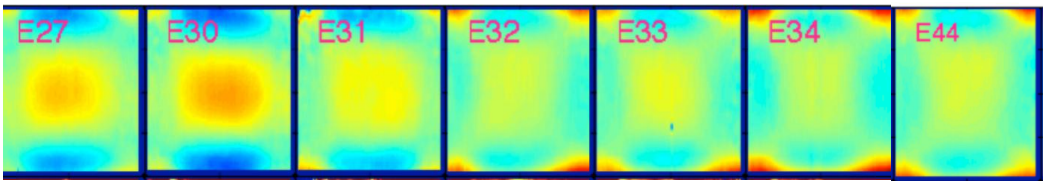

Fig. 11.: The CUP maps of some slumped glass foils, after the subtraction of the cylinder with radius of curvature of 1m, with a linear detrend for each longitudinal line. E27 and E30 are slumped with the light open cover (configuration Fig. 10 left); from E31 the glass foils are slumped with the thick closed cover (configuration Fig. 10 right). Different cooling rate parameters are used for the glass foils from E32 to E44, as shown in Fig. 12.

3) the cooling rate is a key parameter to reduce the mid frequency errors. It was maintained at 9.4°C/h for all glass foils until the PoC#3, included. From the study of the interference fringes between the glass foil and the mould, possible with the slumping cycles performed with the configuration shown in Fig. 10-left, we can state that, after a complete glass-to-mould contact at the soaking temperature (750 °C) with the application of pressure, visible by the absence of interference fringes, we see the reappearance of interference fringes at about 690°C (Fig. 2-right), close to the strain temperature of the Eagle glass, T_{strain} = 669 °C, being this the evidence of the glass transition. We have therefore reduced the cooling rate to 4 and 2.5 °C/h in the region around 690 °C, and we have measured a subsequent decrease in mid frequencies (Fig. 12-right).
Figs. 12 show the effect of the cover and the cooling rate, reducing the sag error and the mid frequency errors respectively. The central scan profile is taken as the most representative, the peripheral region of the MK20-10 being of reduced quality.

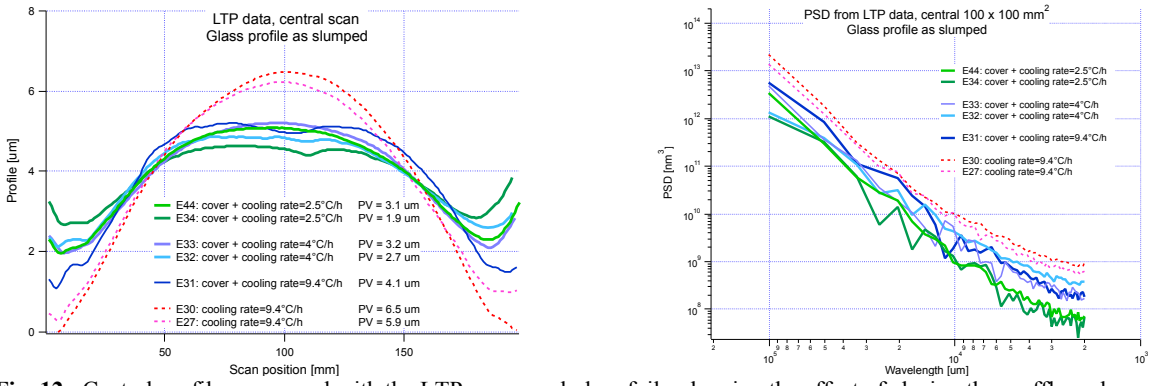

Fig. 12.: Central profiles measured with the LTP on several glass foils, showing the effect of closing the muffle and reducing the cooling rate. Left: from the LTP profiles we can see that the closure of the muffle halves the sag error. Right: from the PSD analysis we prove that the reduction of the cooling rate reduces the mid frequency errors.

5. K20 CHARACTERISTICS AND DEVELOPED PROTOCOLS

Due to the poor surface quality of the MK20-10 slumping mould (Fig. 3), a further improvement in the quality of the slumped glass foils could be reached only with the introduction of the re-polished MK20-20B. The past experience with the MK20-10 and MK20-20 endowed us with solutions for two major issues, never reported previously: a deformation of K20 with the first thermal cycles, never observed by Schott (private communication), and residuals from First Contact on the K20 surface, never reported by Photonic Cleaning [17]. We have developed two dedicated protocols to deal with these issues.

5.1 Annealing protocol

During the production of the PoC#2 prototype, we have noticed that the longitudinal profiles of the cylindrical K20 surface (the MK20-10 at the time of PoC#2) were changed from the profiles measured on the as delivered mould. Therefore, when we received the newly polished MK20-20, we have started a campaign of measurements, checking for deformation after a preliminary annealing cycle, and the subsequent slumping cycles. We had to wait for the second re-work and the new measurements on MK20-20B, to define a protocol to stabilize the K20 surface from deformations. We can now confirm that the K20 is changing profiles with the sole thermal cycle, that is without the application of pressure. Nevertheless we have defined a proper annealing cycle, that is the thermal cycle used for the slumping of the glass foils, which is suitable to prevent further deformation during the subsequent slumpings with pressure. Despite the repeatability of the protocol could not be proven on different moulds in incoming, for cost reasons on the mould's procurement and polishing, the shape stability after several slumping cycles with pressure was proven on MK20-20B.
In Fig. 13 we show the LTP longitudinal profiles of the MK20-20B mould, measured with steps of 1 mm in the longitudinal direction and every cm in the azimuthal direction. The profiles obtained from the as delivered mould are compared to the ones measured after the annealing cycle, evidencing important changes. Nevertheless, our integration procedure is efficiently damping for low frequency errors [8]; therefore this modification, despite being relevant, is not critical for our Slumped Glass Optics technology. On the other hand, no relevant changes were measured on the mid

frequencies. This can be seen in Fig. 14 where the HEWs, computed from physical optics, are shown both for the raw data and for the data after the subtraction of the 8th order best fit polynomial, in order to evidence mid frequency errors. In Fig. 14-right we have over-plotted the HEWs computed from the LTP data after the first slumping with pressure (glass code E46), showing no relevant difference.

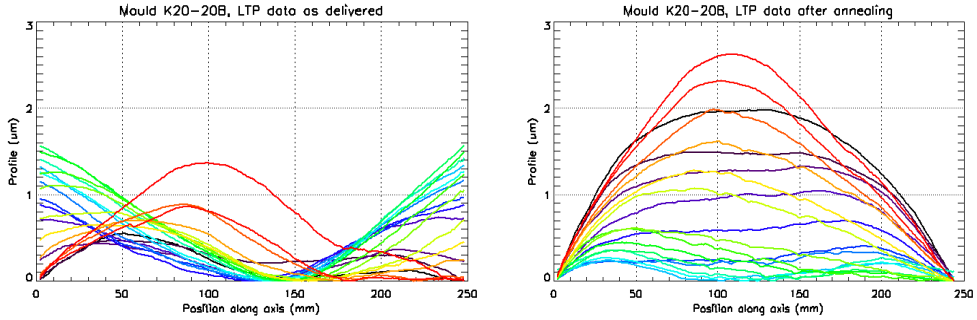

Fig. 13. LTP profiles of the MK20-20B, taken with steps of 1 mm in the longitudinal direction and every cm in the azimuthal direction. Left graph shows the as delivered mould: PV_{center} = 1.4 µm concave, $PV_{90mm\text{-}left}$ = 0.6 µm concave, $PV_{90mm\text{-}right}$ = 0.9 µm convex. Right graph shows the mould after the annealing for comparison: PV_{center} = 0.3 µm concave, $PV_{90mm\text{-}left}$ = 2.1 µm convex, $PV_{90mm\text{-}right}$ = 2.5 µm convex.

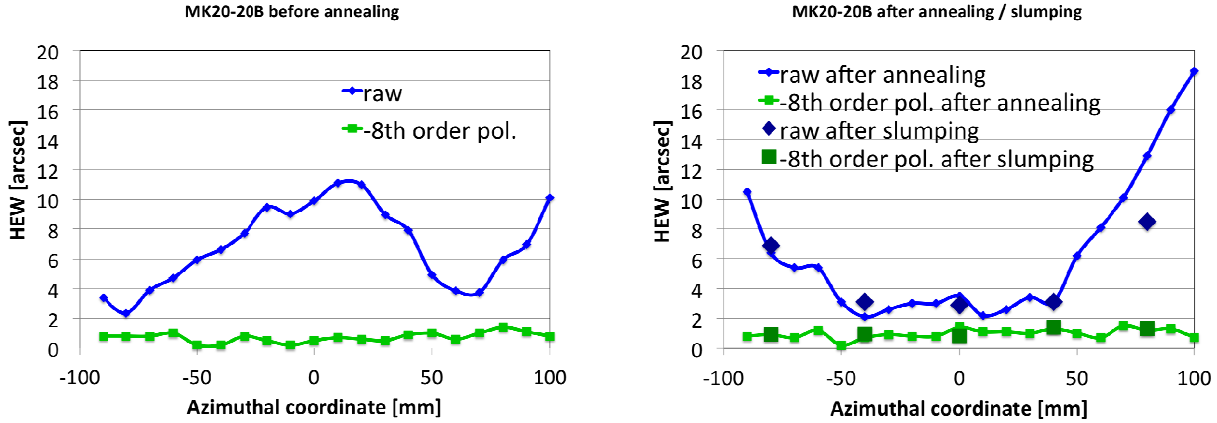

Fig. 14. HEW computed from LTP data with physical optics, on MK20-20B. Both the LTP raw data (blue curve) and the residual after the subtraction of the 8th order best fit polynomial (red curve) are shown. Left is for the as delivered mould, right is for the mould after the annealing. On the right graph the HEWs computed from the LTP data after the first slumping with pressure (glass code E46) are over-plotted, showing no relevant difference.

5.2 Cleaning protocol before slumping

We routinely clean the glass foils and the mould, before their introduction into the furnace for the slumping cycle. Moreover we paint the two surfaces with a First Contact coating, to be stripped just before bringing the glass in contact with the mould inside the muffle, hence removing the dust present on the two surfaces. The First Contact is guaranteed to be a residual free paint [17] and we have proven this to be true on the smooth surface of the glass foil. Anyway, at the mould side, several peaks are present [9] which make the First Contact more difficult to be stripped without residuals. Therefore, after the slumping, the mould surface needs to be cleaned. With the introduction of the MK20-20 and MK20-20B, we could define a cleaning protocol effective in removing the residuals entrapped into the rough mould surface: our protocol foresees the cleaning with a detergent, acetic acid and hydrogen peroxide. AFM measurements on the mould were done (Fig. 15) to compare the surface after the annealing cycle (blue curve), that is before any slumping, and after

the slumping of a glass foil: the measurements taken on the un-cleaned (red curve) and cleaned (green curve) mould surface show that our cleaning protocol is effective in returning to the pristine surface quality.

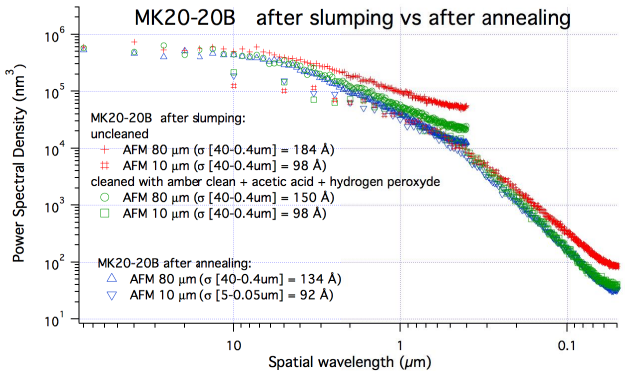

Fig. 15. PSD from AFM 80 and 10 μm scans on MK20-20B. Blue curve is for the mould after the annealing, that is before any slumping and any use of First Contact; red curve is after a glass foil slumping cycle but without the cleaning protocol; green curve is after the slumping and after the cleaning protocol. This last PSD matches the PSD of the pristine mould.

This cleaning protocol was found effective in removing, from the mould surface, entrapped residuals that were seen as repetitive defects in consecutive slumped glass foils, as can be seen in Fig. 16.

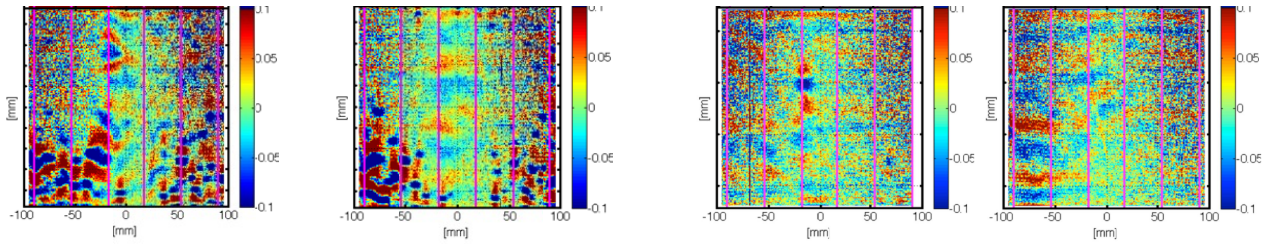

Fig. 16.: CUP maps of consecutive slumped glass foils, after removing the Legendre polynomials up to the 8th order. Left: on MK20-20 before the introduction of the mould cleaning protocol; right: on MK20-20B after the introduction of the mould cleaning protocol

5.3 Alternative solutions against the K20 deformation

Despite the K20 deformation is not critical for our technology, as our integration procedure efficiently corrects for low frequency errors on the shape of the slumped glass foils, it would be preferable to avoid the profile changes of the K20 with the first thermal cycle. This would be essential for those technologies that are using a stress free integration concept and therefore need to produce slumped glass foils with precisely figured Wolter I profiles. The production of our K20 moulds was obtained after polishing cycles following the grinding. We suggest the possibility to perform an annealing cycle just before starting the polishing phase: the idea is to stabilize the K20 surface before starting the fine figuring of the mould. This needs to be checked by experiments.

Alternatively we suggest the use of Silicon Nitride as slumping mould material. We have already performed several tests on Si_3N_4 flat slumping moulds: no deformation was detected and no sticking ever occurred with different temperatures and pressures around the nominal ones, proving this material to be a good candidate for the slumping technique [12]. The research on the Silicon Nitride, as a material for the slumping moulds, was driven by three key points: a higher rigidity with respect to the Zerodur K20 (Young's Modulus for Si_3N_4 = 300 GPa, for K20 = 84.7 GPa), a better matching of the CTE with the one of the glass ($CTE_{Si3N4} = 3.4\times10^{-6}$/ºK, $CTE_{Eagle} = 3.17\ 10^{-6}$/ºK), and a higher thermal conductivity (k) with respect to the Zerodur K20 (k_{Si3N4} = 33 W/mK, k_{K20} =1.63 W/mK). The rigidity of this material makes also

possible to produce a cylindrical slumping mould thinner than the mould in K20, thus reducing the cost of the mould production. As following step, the polishing properties of this material need to be investigated.

6. SLUMPING ON RE-POLISHED MK20-20B

Four slumped glass foils were slumped on the re-polished MK20-20B, with the process parameters optimized on MK20-10. For the first time, we could measure and compare the mid frequency errors on the slumped glass foils and the slumping mould. Fig. 17 shows the central portion of a LTP scan line, 45 mm off the center: this is a very good result in mould replication, never reached before. As shown in Fig. 14, these errors account for about 1 arcsec in the final HEW.

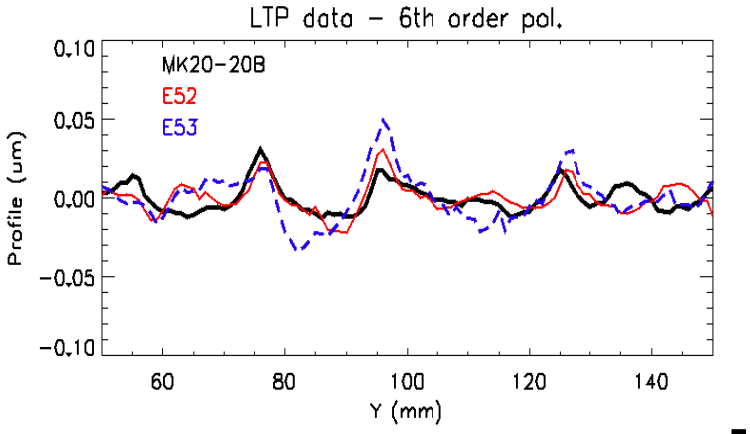

Fig. 17.: The LTP data, of one longitudinal scan profile, after the subtraction of the 6th order best fit polynomial. The mid frequency errors of the MK20-20B mould are replicated on the slumped glass E52 and E53.

We here want to compare the results of the glass foils produced on the MK20-20B (glass code E52-E53-E54-E55) with the ones integrated into the prototypes PoC#3 and PoC#4. In Table 2, the main characteristics of these slumped glass foils are listed. In Fig. 18 we compare the CUP maps of three slumped glass foils, one out of each group of Table 2: the process parameters defined during this research activity were effective in maintaining the low sag error when moving from MK20-10 to MK20-20B.

Table 2: Main characteristics and process conditions of the slumped glass foils integrated into the prototypes PoC#3 and PoC#4, compared with the most recent results

		PoC#3	**PoC#4**	**Present**
Year		2014	Early 2015	Present
Slumping mould		MK20-20	MK20-10	MK20-20B
Slumped glass material		Eagle	Eagle	Eagle
Slumped glass foils code		E16-E18	PP3: E5-E9 PP2: E27-E30 PP1: E32-E34 PP0: E33-E35	E52-E53 E54-E55
K20 new cleaning protocol		no	yes	yes
Mould height		2.5 mm	1.1 mm	1.1 mm
Thick closed muffle cover		no	no: E5-E9-E27-E30 yes: E32-E33-E34 thin flat cover: E35	yes
Soaking time		4h	4h	4h
Cooling rate	from 722 to 600 °C	9.4°C/h	9.4°C/h: E5-E9-E27-E30	
	from 722 to 670 °C		4°C/h: E32-E33 2.5°C/h: E34	2.5°C/h

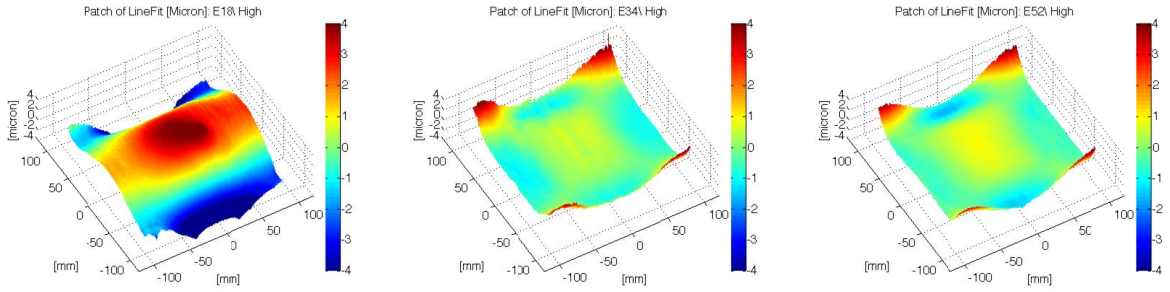

Fig. 18. CUP maps of some slumped glass foils: residual with respect of a linear fit along the optical axis, at different azimuthal coordinates. The vertical scale is in μm. Left: a glass foil integrated into the PoC#3 (glass code E18, central sag error ~ 10 μm); Center: a glass foil integrated into the PoC#4 (glass code E34, central sag error ~ 2 μm); Right: a glass foil recently slumped on MK20-20B (glass code E52, central sag error ~ 3 μm)

The expected HEWs computed from physical optics in single reflection, from the LTP scans taken on the glass foils shown in Fig. 18, after the simulation of a perfect integration, are presented in the following figure. The net decrease of the HEW computed from the central scan (E34 and E52) is the result of the sag error reduction, while the decrease in the HEW computed from the lateral profiles (E18 and E52) is the effect of the new K20 with no surface defect in the cm scale, visible in Fig. 3.

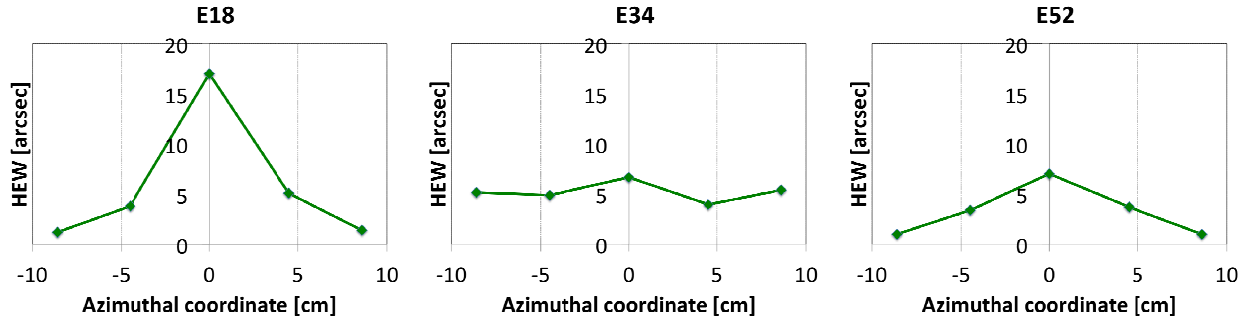

Fig. 19 the HEW expected from the LTP glass profiles, obtained with physical optics from the integrated profiles of Fig. 18. The glass foils represents the PoC#3, PoC#4 and the present result, respectively.

Finally, the trend in the HEWs, computed for the slumped glass foils during the last 2 years, is presented in Fig. 20, showing that the last four glass foils, slumped on MK20-20B (glass code E52-E53-E54-E55), have almost reached our goal of 2 arcsec computed from shape data in single reflection.

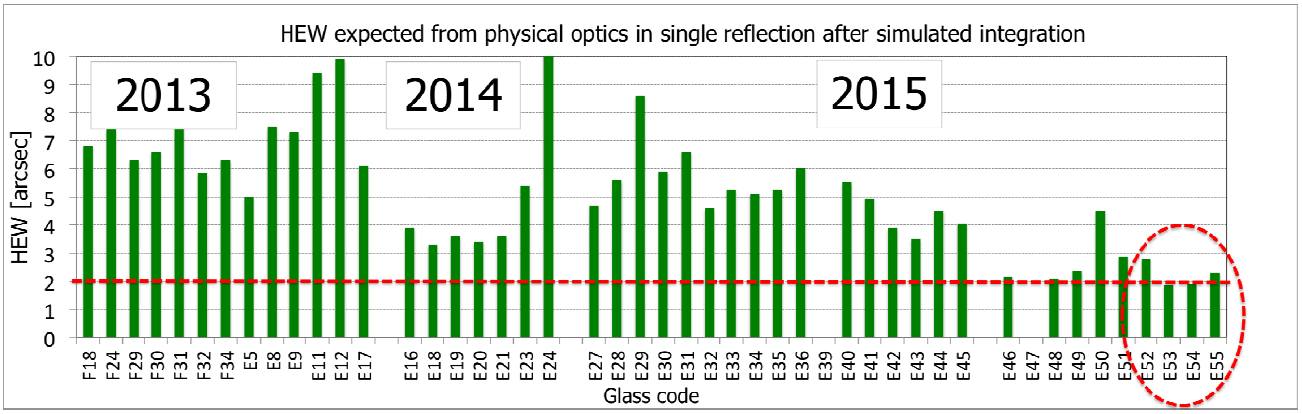

Fig. 20 Trend of the HEWs expected from the LTP slumped glass profiles, obtained with physical optics in single reflection after the simulation of a perfect integration. The last four glass foils (glass code E52-E53-E54-E55) returns expected HEWs of less than 3 arcsec.

For what concerns the roughness, the partial replication of the mould high frequency features (Fig. 4) guarantees our goal of HEW contribution from roughness less than 1 arcsec at 1 keV.

We are now working on reducing the pressure in order to reduce the roughness of the slumped glass foils, keeping the mid frequency to an acceptable level. Slumping with P = 30 g/cm^2, resulted in a better glass roughness quality but a portion of the glass foil was deformed by an air bubble. We therefore conducted tests keeping P = 50 g/cm^2 only for 1h, to remove all the air present, and reducing it to P = 30 g/cm^2 for the rest of the cooling cycle, while keeping the pressure control in closed loop (E51, blue curve of Fig. 21). The result in roughness was at the level of the POC#3 glass foils, but the sag reduction was not as good as with P = 50 g/cm^2 in open loop. We are now studying other ways of controlling the pressure in order to improve the result.

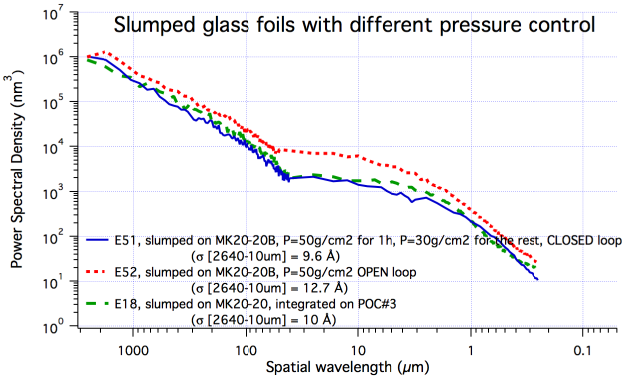

Fig . 21. Roughness PSD comparison of glass foils slumped on MK20-20 and MK20-20B with different pressure control.

7. CONCLUSIONS

In this paper we have presented the step forwards in our slumping technology assisted by pressure. The driving idea of the research activity was the reduction of the sag errors, which was still too high at the time of the PoC#2 and PoC#3 prototypes. Several modification in the process were implemented in the PoC#4 prototype, leading to a reduction of the central sag error from about 10 to 2 μm. Beside that other process changes were implemented leading to a further improvement also in the mid to high frequency range. The mould height was optimized with Finite Element Analysis and experiments; the muffle was closed to reduce the thermal gradients; the cooling rate were decreased; a new protocol

for cleaning the mould surface before slumping was introduced, in order to avoid repetitive spots at subsequent slumping cycles. After the re-polishing of the Zerodur K20 mould, we have proven to be able to obtain glass foils with small sag error also on a smooth K20 surface, and therefore we have solved the problem encountered in the production of the PoC#3. Moreover we have obtained the best result, up to now, in overall quality of the glass foils, having produced four slumped glass foils on the re-polished K20 with expected HEW, computed from physical optics in single reflection after the simulation of a perfect integration, of almost 2 arcsec, which was our goal. With the improved mould replication, we are now for the first time reached a point where we partially replicate the mid frequency features on the mould. From the point of view of roughness, the contribution to the HEW, of the slumped glass foils, is guaranteed to be less then 1 arcsec at 1 keV. In order to go to higher X-ray energies, the next activity will foresee further work to reduce the roughness replication from the mould to the glass foils.

ACKNOWLEDGMENTS

We kindly thank Giorgio Pariani for his valuable support with the ZYGO measurements. We also appreciated all the efforts of the Hellma Optics company in improving the quality on the K20 mould.

REFERENCES

[1] Nandra, K., Barcons, X., Barret, D., Fabian, A., den Herder, J.W., Piro, L., Watson, M., "*Athena: The Advanced Telescope for High Energy Astrophysics. Mission proposal*," http://www.the-athena-x-ray-observatory.eu

[2] Reid, P.B., Aldcroft, T.L., Cotroneo, V., Davis, W., Johnson-Wilke, R.L., McMuldroch, S., Ramsey, B.D., Schwartz, D.A., Trolier-McKinstry, S., Vikhlinin, A., Wilke, R.H.T., "*Development status od adjustable grazing incidence optics for 0.5 arc second X-ray imaging*," Proc. SPIE 8861, 88611Q-2 (2014).

[3] Spiga, D., Barbera, M., Basso. S., Civitani, M., Collura, A., Lo Cicero, U., Lullo, G., Pellicciari, C., Riva, M., Salmaso, B., Sciortino, L., "*Manufacturing and testing a thin glass mirror shell with piezoelectric active control*," Proc. SPIE 9603, (2015).

[4] Civitani, M., Basso, S., Ghigo, G., Pareschi, G., Salmaso, B., Spiga, D., et al., "*X-ray Optical Units made of glass: achievements and perspectives,*" Proc. SPIE 9144, 914416 (2014).

[5] Proserpio, L., Basso, S., Breuning, E., Buratti, E., Burwitz, V., Civitani, M., Eder, J., Friedrich, P., Hartner, G.D., Menz, B., Rohé, C., Winter, A., "*JIM: a join integrated module of glass x-ray optics for astronomical telescopes*," Proc. SPIE 9603, (2015).

[6] Proserpio, L., Civitani, M., Ghigo, M., Pareschi, G., "*Thermal shaping of thin glass substrates for segmentes grazing incidence active optics*," Proc. SPIE 7803, 78030K-2 (2010)

[7] Jimenez-Garate, M. A., Hailey, C. J., Craig, W. W., Christensen, F. E., "*Thermal forming of glass microsheets for x-ray telescope mirror segments,*" Applied Optics 42, 4 (2003)

[8] Parodi, G., Martelli, F., Basso, S., Citterio, O. Civitani, M., Conconi, P., Ghigo, M., Pareschi, G., Zambra, A., **"***Design of the IXO optics based on thin glass plates connected by reinforcing ribs,*" Proc. SPIE 8147, 81470Q (2011)

[9] Salmaso, B., Basso, S., Brizzolari, C., Civitani, M.M., Ghigo, M., Pareschi, G., et al., "*Production of thin glass mirrors by hot slumping for X-ray telescopes: present process and ongoing development*," Proc SPIE 9151, 91512W (2014)

[10] Winter, A., Breunig, E., Friedrich, P., Proserpio, L., Dohring, T., "*Indirect glass slumping for future x-ray missions: overview, status, progress*," Proc. SPIE 9063, this conference (2015)

[11] Cotroneo, V., Davis, W.N., Reid, P.B., Schwartz, D.A., Trolier-McKinstry, S., Wilke, R.H.T., "*Adjustable grazing incidence x-ray optics: measurement of actuator influence functions and comparison with modeling,*" Proc. SPIE 8147, 81471R (2011)

[12] Salmaso, B., Basso, S., Brizzolari, C., Civitani, M., Ghigo, M., Pareschi, G., Spiga, D., Tagliaferri, G., Vecchi, G., "*Direct hot slumping of thin glass foils for future generation X-ray telescopes: current state of the art and future outlooks,*" Proc. ICSO, (2014)

[13] Ghigo, M. , Basso, S. , Borsa, F., Bavdaz, M., Citterio, O. , Civitani, M. , et al., "*Development of high angular resolution x-ray telescopes based on slumped glass foils*," Proc. SPIE 8443, 84430R (2012).

[14] Civitani, M.M., Basso, S., Ghigo, M., Salmaso, B., Spiga, D., Tagliaferri, G., Vecchi, G., Hartner, G.D., Menz, B., Burwitz, V., Pareschi, G., "*Slumped glass optics based on thin hot formed glass segments and interfacing*

ribs for high angular resolution x-ray astronomy: performances and development status," Proc. SPIE 9603, (2015).
[15] Civitani, M.M., Ghigo, M., Citterio, O. Conconi, P. Spiga, D. Pareschi, G. Proserpio, L., "*3D characterization of thin glass x-ray mirrors via optical profilometry,"* Proc. SPIE 7803, 78030L (2010)
[16] Raimondi, L., Spiga, D., "*Fresnel diffraction-based computation of point spread functions from metrology*," A&A 573, A22 (2015)
[17] http://www.photoniccleaning.com